

Title	Thermodynamic analysis of ionizable groups involved in the catalytic mechanism of human matrix metalloproteinase 7 (MMP-7).
Author(s)	Takeharu, Hitoshi; Yasukawa, Kiyoshi; Inouye, Kuniyo
Citation	Biochimica et biophysica acta (2011), 1814(12): 1940-1946
Issue Date	2011-12
URL	http://hdl.handle.net/2433/151850
Right	© 2011 Elsevier B.V.
Type	Journal Article
Textversion	author

1 BBA - Proteins and Proteomics

2

3 **Thermodynamic analysis of ionizable groups involved in the catalytic mechanism**
4 **of human matrix metalloproteinase 7 (MMP-7)**

5

6 Hitoshi Takeharu, Kiyoshi Yasukawa, Kuniyo Inouye*

7

8 *Division of Food Science and Biotechnology, Graduate School of Agriculture, Kyoto*
9 *University, Sakyo-ku, Kyoto 606-8502, Japan*

10

11 *Abbreviations:* AMPSO, 3-[(1,1-dimethyl-2-hydroxy-ethyl)amino]-2-
12 hydroxypropane sulfonic acid; DMSO, dimethyl sulfoxide; HEPES,
13 2-[4-(2-hydroxyethyl)-1-piperazinyl] ethanesulfonic acid; K_e , proton dissociation
14 constant; MES, 2-(*N*-morpholino)ethanesulfonic acid; MMP, matrix metalloproteinase;
15 MOCAc-PLG, (7-methoxycoumarin-4-yl)acetyl-L-Pro-L-Leu-Gly; MOCAc-
16 PLGL(Dpa)AR, (7-methoxycoumarin-4-yl)acetyl-L-Pro-L-Leu-Gly-L-Leu-[*N*³-(2,4-
17 dinitrophenyl)-L-2,3-diaminopropionyl]-L-Ala-L-Arg-NH₂.

18 *Correspondence author. Tel.: +81 75 753 6266; fax: +81 75 753 6265. *E-mail*
19 *address:* inouye@kais.kyoto-u.ac.jp

20 *Keywords:* ionizable group; matrix metalloproteinase; MMP-7; proton dissociation
21 constant; thermodynamic analysis.

22

23

24

25 **Abstract**

26

27 Human matrix metalloproteinase 7 (MMP-7) exhibits a broad bell-shaped
28 pH-dependence with the acidic and alkaline pK_e (pK_{e1} and pK_{e2}) values of about 4 and
29 10. In this study, we estimated the ionizable groups involved in its catalytic mechanism
30 by thermodynamic analysis. pK_a of side chains of L-Asp, L-Glu, L-His, L-Cys, L-Tyr,
31 L-Lys, and L-Arg at 25-45°C were determined by the pH titration of amino-acid
32 solutions, from which their enthalpy changes, ΔH° , of deprotonation were calculated.
33 pK_{e1} and pK_{e2} of MMP-7 at 15-45°C were determined in the hydrolysis of
34 (7-methoxycoumarin-4-yl)acetyl-L-Pro-L-Leu-Gly-L-Leu-[N^3 -(2,4-dinitrophenyl)-L-2,3-
35 diaminopropionyl]-L-Ala-L-Arg-NH₂, from which ΔH° for pK_{e1} and pK_{e2} were
36 calculated. The ΔH° for pK_{e1} ($-20.6 \pm 6.1 \text{ kJ mol}^{-1}$) was similar to that for L-Glu ($-23.6 \pm$
37 5.8 kJ mol^{-1}), and the ΔH° for pK_{e2} ($89.9 \pm 4.0 \text{ kJ mol}^{-1}$) was similar to those for L-Arg
38 ($87.6 \pm 5.5 \text{ kJ mol}^{-1}$) and L-Lys ($70.4 \pm 4.4 \text{ kJ mol}^{-1}$). The mutation of the active-site
39 residue Glu198 into Ala completely abolished the activity, suggesting that Glu198 is the
40 ionizable group for pK_{e1} . On the other hand, no arginine or lysine residues are found in
41 the active site of MMP-7. We proposed a possibility that a protein-bound water is the
42 ionizable group for pK_{e2} .

43

44

45

46 **1. Introduction**

47

48 Human matrix metalloproteinase 7 (MMP-7, Matrilysin) [EC 3.4.24.23] is the
49 smallest matrix metalloproteinase (MMP), lacking a carboxyl terminal hemopexin-like
50 domain conserved in common MMPs. It is believed to play an important role in tumor
51 invasion and metastasis [1, 2]. The molecular mass of the latent pro-form is 28 kDa, and
52 that of its mature form is 19 kDa [3]. MMP-7 is composed of a five-stranded β -sheet
53 and three α -helices, and contains a zinc ion essential for activity and other zinc and
54 calcium ions that are considered necessary for stability [4]. Like all other MMPs, it has
55 the consensus sequence HEXXHXXGXXH, in which three histidine residues chelate a
56 catalytic zinc ion, and a methionine-containing turn (Met-turn). Hence, it is grouped in
57 clan MA(M) [5]. In recent years, target molecules through which MMP-7 exerts
58 biological functions have become apparent, such as heparin [6], heparan sulfate [6],
59 cholesterol sulfate [7-9], and ErbB4 receptor [10]. The inhibitions of MMP-7 activity by
60 natural compounds [11,12], synthetic compounds [13], and detergents [14] were
61 reported.

62 Generally, ionizable groups involved in the catalytic mechanisms of enzyme are
63 estimated from the three-dimensional structure and pK_e values. Figure 1A shows the
64 structure of MMP-7-hydroxamate inhibitor complex [4]. In this study, the numbering of
65 amino acid residues of pro-MMP-7 is according to the previous report [15], in which the
66 mature MMP-7 begins at Tyr78. MMP-7 has three α helices and five β strands [4].
67 Tyr193 and Glu198 are located at the second α -helix (Leu192-Leu203), while Tyr216
68 and Tyr219 are located at the Met-turn (Pro211-Gly222). Sequence comparison of
69 MMP-1 [16], MMP-2 [17], MMP-3 [18], MMP-7 [19], MMP-8 [20], MMP-9 [21],

70 MMP-10 [19], MMP-11 [22], MMP-12 [21], MMP-13 [21], and MMP-14 [23] revealed
71 that Glu198 and Tyr219 are conserved in all MMPs, while Tyr216 is conserved in
72 several MMPs, and Tyr193 is unique to MMP-7 [24]. Tyr219 and Tyr216 form the S1'
73 subsite. MMP-7 exhibits a broad bell-shaped pH-dependence with the acidic and
74 alkaline pK_e (pK_{e1} and pK_{e2}) values of about 4 and 10 [13,25]. As a result, three
75 ionization forms of MMP-7 and MMP-7-substrate complex are considered, respectively
76 (Fig. 2). Glu198 and Tyr219 are believed to be the ionizable groups responsible for pK_{e1}
77 and pK_{e2} , respectively. However, Cha *et al.* proposed that the zinc-bound water might be
78 the ionizable group responsible for pK_{e1} [26]. We found that the MMP-7 whose tyrosyl
79 residues were nitrated with tetranitromethane retained activity [27]. In addition, we
80 recently demonstrated that all Tyr219 variants retained activity [28]. These results
81 indicate that Tyr219 is not critical for catalytic activity. We also demonstrated that
82 Tyr193 and Tyr216 variants retained activity [28].

83 One of the critical problems with using pK_a values of free amino acids for
84 estimation of charge states of amino acid residues is that little water (and hence protons)
85 is available for the residues buried in a protein core, while large amounts of water (55 M
86 water) is available for the residues facing bulk solution. In 1930-1960, enthalpy changes,
87 ΔH° , of deprotonation of side chains of amino acid residues were determined by the
88 measurement of pH- and temperature-dependences of electromotive force of the battery
89 containing amino acids, dipeptides, or tripeptides in a cell [29-33]. It was demonstrated
90 that in dipeptides and tripeptides, ΔH° values of side chains of amino acid residues are
91 not affected by the amino acid residues in their neighborhoods and are almost equal to
92 the ΔH° values of side chains of free amino acids [29-33]. Therefore, ΔH° values can be
93 used as a clue to estimate the ionizable groups in the catalytic mechanism of enzymes

94 [29,34-36]. However, compared with the estimation of the ionizable groups with pK_e
95 values, the estimation with ΔH^0 values is not commonly used. This might be due to that
96 reliable ΔH^0 values of side chains of amino acid residues have not been available. In this
97 study, we determined the ΔH^0 of side chains of amino acid residues by the pH-titration
98 of amino-acid solutions and used them to estimate the ionizable groups involved in the
99 catalytic mechanism of MMP-7.

100

101 **2. Materials and methods**

102

103 *2.1. Materials*

104

105 (7-methoxycoumarin-4-yl)acetyl-L-Pro-L-Leu-Gly-L-Leu-[N^3 -(2,4-dinitrophenyl)-
106 L-2,3-diaminopropionyl]-L-Ala-L-Arg-NH₂ [MOCAC-PLGL(Dpa)AR] (Lot 491214,
107 molecular mass 1093.2 Da) [37] and (7-methoxycoumarin-4-yl)acetyl-L-Pro-L-Leu-Gly
108 (MOCAC-PLG) (Lot 510913, molecular mass 501.54 Da) were purchased from the
109 Peptide Institute (Osaka, Japan). Their concentrations were determined by the denoted
110 weight and the molecule weight.
111 3-[(1,1-Dimethyl-2-hydroxy-ethyl)amino]-2-hydroxypropane sulfonic acid (AMPSO,
112 Lot 9355C, molecular mass 227.3 Da) and L-Glu (Lot TLE5153) were from Wako Pure
113 Chemical (Osaka). L-Asp (Lot 115H0563) and N^α -acetyl-L-Lys (Lot A1020) were from
114 Sigma (St. Louis, MO, USA). L-His (Lot M2N7937), L-Cys (Lot M7H2081), L-Tyr,
115 (Lot M7K3391), and L-Arg (Lot M7K6540) were from Nacalai Tesque (Kyoto, Japan).
116 All other chemicals were from Nacalai Tesque.

117

118 2.2. *Expression and purification of MMP-7*

119

120 Expression in *Escherichia coli* and purification of recombinant MMP-7 were
121 carried out, as described previously [31,39]. Briefly, mature MMP-7 (Met77-Lys250)
122 was expressed in BL21(DE3) cells in the forms of inclusion bodies, solubilized with 6
123 M guanidine HCl, refolded with 1 M L-arginine, and purified by sequential ammonium
124 sulfate precipitation and heparin affinity column-chromatography procedures of the
125 refolded products. The concentration of MMP-7 was determined spectrophotometrically
126 using the molar absorption coefficient at 280 nm, ϵ_{280} , of 31,800 M⁻¹ cm⁻¹ [38].
127 Site-directed mutagenesis was carried out using QuikchangeTM site-directed
128 mutagenesis kit (Stratagene, La Jolla, CA) for construction of E198A, A162G, and
129 P217G. The nucleotide sequences of mutated MMP-7 genes were verified by a
130 Shimadzu DNA sequencer DSQ-2000 (Kyoto).

131

132 2.3. *Fluorometric analysis of hydrolysis of MOCAC-PLGL(Dpa)AR*

133

134 The MMP-7-catalyzed hydrolysis of MOCAC-PLGL(Dpa)AR was initiated by
135 mixing 1222 μ l of the reaction buffer, 20 μ l of the MMP-7 solution (625 nM), and 8 μ l
136 of the substrate solution (234 μ M) dissolved in DMSO. The initial concentrations of
137 enzyme, MOCAC-PLGL(Dpa)AR, and DMSO were 10 nM, 1.5 μ M, and 0.64% (v/v),
138 respectively. The reaction buffers were 50 mM acetate-NaOH buffer at pH 3.6-5.8, 50
139 mM MES-NaOH buffer at pH 5.6-7.0, 50 mM HEPES-NaOH buffer at pH 6.8-8.6, and
140 50 mM AMPSO-NaOH buffer at pH 8.6-10.4, each containing 10 mM CaCl₂. The
141 reaction was measured by following the increase in the fluorescence intensity at 393 nm

142 with excitation at 328 nm with a JASCO FP-777 fluorescence spectrophotometer
 143 (Tokyo, Japan). The peptide bond of Gly-L-Leu residues was cleaved by MMP-7, and
 144 the amount of the product MOCAC-PLG was estimated by the fluorescence intensity by
 145 comparison with the fluorescence intensity of an authentic MOCAC-PLG solution. The
 146 hydrolysis was carried out under pseudo-first order conditions, where the initial
 147 concentration of MOCAC-PLGL(Dpa)AR (1.5 μ M) was much lower than K_m (60 μ M)
 148 [38]. The Michaelis-Menten equation is, then, expressed as Eq. 1.

149

$$150 \quad v_o = (k_{cat}/K_m)[E]_o[S]_o \quad (1)$$

151

152 where v_o , k_{cat} , $[E]_o$, and $[S]_o$ mean the initial reaction rate, the molecular activity, the
 153 initial enzyme concentration, and the initial substrate concentration, respectively. The
 154 kinetic parameters, the intrinsic k_{cat}/K_m , $(k_{cat}/K_m)_o$, and the proton dissociation constants
 155 (K_{e1} and K_{e2}) for pH-dependence of the activity were calculated from Eq. 2 by a
 156 non-linear least squares regression method with Kaleida Graph Version 3.5 (Synergy
 157 Software, Essex, VT).

158

$$(k_{cat}/K_m)_{obs} = \frac{(k_{cat}/K_m)_o}{1 + \frac{[H^+]}{K_{e1}} + \frac{K_{e2}}{[H^+]}} \quad (2)$$

159

160 In this equation, $(k_{cat}/K_m)_{obs}$ and $[H]$ mean the k_{cat}/K_m value observed and the proton
 161 concentration, respectively, at the specified pH.

162

163 *2.4. Thermodynamic analysis of K_{e1} and K_{e2}*

164

165 The enthalpy changes, ΔH° , of deprotonation were calculated from pK_e shifts using
166 Eq. 3, known as the van't Hoff equation,

167

$$\frac{d(\ln K_e)}{dT} = \frac{\Delta H^\circ}{RT^2} \quad (3)$$

168

169 where T and R mean the absolute temperature in degrees Kelvin and the gas constant (=
170 $8.314 \text{ J K}^{-1} \text{ mol}^{-1}$), respectively. When this equation is integrated, it is expressed as Eq.
171 4,

172

$$-\log K_e = \frac{\Delta H^\circ}{2.303 RT} + A \quad (4)$$

173

174 where A means the constant of integration. Thus, a slope of a plot for pK_e values versus
175 $1/T$ gives ΔH° .

176

177 *2.5. Titration of pH of amino-acid solution and thermodynamic analysis of proton*
178 *dissociation constant of side chains of amino acids*

179

180 Amino acid was dissolved in water to be 10 mM for L-Asp, L-Glu, L-His, L-Cys,
181 and L-Arg and 1 mM for L-Tyr and N^α -acetyl-L-Lys. Titration was made with 50 or 100
182 μl of 2 M HCl or 2 M NaOH for each amino-acid solution (500 ml) incubated at 25, 35,
183 or 45°C as follows: the L-Asp and L-Glu solutions were titrated with NaOH until pH
184 reached 6.0. The L-His solution was titrated with HCl until pH reached 3.0. The L-Cys
185 solution was titrated with HCl until pH reached 6.8. The L-Arg solution was titrated

186 with HCl until pH reached 9.8. The L-Tyr solution was titrated with HCl until pH
 187 reached 7.5. The N^α -acetyl-L-Lys solution was titrated with HCl until pH reached 9.2.

188 The following is the case with L-Glu, as an example. Based on the previous reports
 189 that pK_a values of α -COOH and γ -COOH of L-Glu at 25°C are around 2.0 and 4.0,
 190 respectively [29-33], the course of a titration of L-Glu with NaOH from pH 2 to 6 can
 191 be represented in the following schemes.

192



195

196 The degree of dissociation, α , is defined as the following equation,

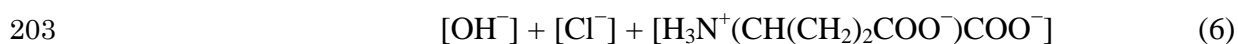
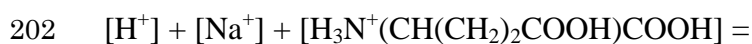
197

$$\alpha = \frac{2[H_3N^+(CH(CH_2)_2COO^-)COO^-] + [H_3N^+(CH(CH_2)_2COOH)COO^-]}{C} \quad (5)$$

198

199 where C means the initial concentration of L-Glu. The α value increases up to 2 in the
 200 course of the titration. The electric balance is given by the following equation.

201



204

205 Substituting Eq. 5 into Eq. 6 yields the following equation,

206

207

$$\alpha = \frac{C - [H^+] + [Na^+] - K_w/[H^+] - [Cl^-]}{C} \quad (7)$$

208

209 where K_w is ionic product. The α at each pH was calculated from Eq. 7. K_{a1} and K_{a2} ,
 210 which are defined as Eqs. 8 and 9, respectively, were calculated from Eq. 10 by a
 211 non-linear least squares regression method with Kaleida Graph Version 3.5.

212

$$K_{a1} = \frac{[H^+] [H_3N^+(CH(CH_2)_2COOH)COO^-]}{[H_3N^+(CH(CH_2)_2COOH)COOH]} \quad (8)$$

213

$$K_{a2} = \frac{[H^+] [H_3N^+(CH(CH_2)_2COO^-)COO^-]}{[H_3N^+(CH(CH_2)_2COOH)COO^-]} \quad (9)$$

214

$$\alpha = \frac{2 + \frac{[H^+]}{K_{a2}}}{1 + \frac{[H^+]}{K_{a2}} + \frac{[H^+]^2}{K_{a1} K_{a2}}} \quad (10)$$

215

216 ΔH° of deprotonation of side chains of L-Glu was calculated from pK_{a2} shift using Eq. 3.

217

218 3. Results

219

220 3.1. ΔH° values of deprotonation of side chains of amino acids

221

222 The wild-type MMP-7 was prepared as described in Materials and methods section.
 223 Starting with 100 ml of *E. coli* cultures, 2 mg purified enzyme was recovered. Upon
 224 SDS-PAGE under reducing conditions, each yielded a single band with a molecular

225 mass of 19 kDa (data not shown).

226 To determine ΔH° values of deprotonation of side chains of amino acids, we made
227 a titration of pH of L-Asp, L-Glu, L-His, L-Cys, L-Tyr, N^α -acetyl-L-Lys, and L-Arg
228 solutions. The result with L-Glu is shown in Fig. 3, as an example. The degree of
229 dissociation, α , which is defined as Eq. 5, increased rapidly with an increase of pH from
230 1.9 to 2.5, gradually with the increase from 2.5 to 3.8, and rapidly again with the
231 increase from 3.8 to 4.5. The pK_{a1} and pK_{a2} were calculated by Eq. 10 to be 2.1 ± 0.1
232 and 4.0 ± 0.1 for 25°C, 2.2 ± 0.1 and 4.1 ± 0.1 for 35°C, and 2.3 ± 0.1 and 4.2 ± 0.1 for
233 45°C, respectively. The pK_{a1} was assigned to α -carboxyl group, and the pK_{a2} was
234 assigned to the side chain of L-Glu, based on the previous reports [29-33]. ΔH° for the
235 pK_{a2} was calculated by the van't Hoff plot to be $-23.6 \pm 5.8 \text{ kJ mol}^{-1}$ (inset of Fig. 3). All
236 results are summarized in Table 1. The ΔH° of the side chains of L-Asp and L-Glu were
237 negative, while those of the other five positive. The ΔH° of the side chains of L-Asp,
238 L-His, and L-Cys were almost the same as the ones previously reported, which were
239 determined by measuring the pH- and temperature-dependences of electromotive force
240 of the battery containing amino acids or dipeptides in the cell (-6 to 6 kJ mol^{-1} for L-Asp
241 [29], 29 - 32 kJ mol^{-1} for L-His [31], and 24 - 26 kJ mol^{-1} for L-Cys [33]). On the other
242 hand, the ΔH° of the side chains of the other four were substantially different from the
243 ones previously reported (-6 to 6 kJ mol^{-1} for L-Glu [29], 25 - 26 kJ mol^{-1} for L-Tyr [31],
244 44 - 55 kJ mol^{-1} for L-Lys [31], and 50 - 52 kJ mol^{-1} for L-Arg [31]).

245

246 *3.2. ΔH° of deprotonation of ionizable groups responsible for pK_{e1} and pK_{e2} of MMP-7*

247

248 According to Fig. 2 and Eq. 2, the pH dependence of k_{cat}/K_m results from the

249 association and dissociation of proton in the free MMP-7, but not the MMP-7 combined
250 with substrate. The $k_{\text{cat}}/K_{\text{m}}$ values of MMP-7 in the hydrolysis of
251 MOCAc-PLGL(Dpa)AR in the pH range of 3.6-10.4 at 15, 25, 35, and 45°C were
252 determined by Eq. 1 and are shown in Fig. 4. All plots showed bell-shaped curves. The
253 plot at 15°C showed the widest active pH-range while that at 45°C showed the
254 narrowest. The intrinsic $k_{\text{cat}}/K_{\text{m}}$, $(k_{\text{cat}}/K_{\text{m}})_0$, and the $\text{p}K_{\text{e}}$ values were determined by Eq. 2,
255 which are summarized in Table 2. The $(k_{\text{cat}}/K_{\text{m}})_0$ value was the lowest at 15°C and the
256 highest at 45°C. Figure 5 shows van't Hoff plot for $\text{p}K_{\text{e}1}$ and $\text{p}K_{\text{e}2}$. ΔH° of deprotonation
257 were calculated to be $-20.6 \pm 6.1 \text{ kJ mol}^{-1}$ for $\text{p}K_{\text{e}1}$ and $89.9 \pm 4.0 \text{ kJ mol}^{-1}$ for $\text{p}K_{\text{e}2}$.

258

259 *3.3. Estimation of the ionizable groups responsible for $\text{p}K_{\text{e}1}$ and $\text{p}K_{\text{e}2}$ of MMP-7*

260

261 By comparison with the ΔH° of MMP-7 ($-20.6 \pm 6.1 \text{ kJ mol}^{-1}$ for $\text{p}K_{\text{e}1}$ and $89.9 \pm$
262 4.0 kJ mol^{-1} for $\text{p}K_{\text{e}2}$) with the ΔH° of side chains of amino acids (Table 1), glutamate
263 residue was thought to be the ionizable group responsible for $\text{p}K_{\text{e}1}$, and arginine or
264 lysine residue for $\text{p}K_{\text{e}2}$. This suggested that Glu198 is the ionizable group for $\text{p}K_{\text{e}1}$ (Fig.
265 1), as previously pointed out [4]. However, no arginine or lysine residues are found in
266 the active site (Fig. 1). We therefore hypothesized that a protein-bound water is the
267 ionizable group for $\text{p}K_{\text{e}2}$.

268

269 *3.4. Water molecules as the candidate for ionizable group responsible for $\text{p}K_{\text{e}2}$*

270

271 The hydroxamate (R-CO-NH-OH) peptide mimetic inhibitor, which binds
272 covalently to the active-site zinc ion, is the first MMP inhibitor [40]. In the

273 MMP-7-hydroxamate inhibitor complex (Protein Data Bank no. 1MMQ) [4], we
274 noticed two water molecules (W1 and W2) as the possible candidates for the ionizable
275 group responsible for pK_{e2} (Fig. 1B), based on the following reasons: (i) W1 and W2 are
276 located 2.7 Å far from each one of the two oxygen atoms of hydroxamate bound to the
277 active site zinc ion; (ii) W1 binds to the main-chain nitrogen atom of Ala162, and W2
278 binds to the main-chain carbonyl oxygen atom of Pro217. Ala162 is located at the fourth
279 β -sheet (Ala162-Ala164) of MMP-7, and Pro217 is located at the Met-turn
280 (Pro211-Gly222). Both Ala162 and Pro217 are conserved among MMPs; and (iii) In the
281 X-ray crystallographic structure of MMP-7 complexed with carboxylate inhibitor
282 (1MMP) and sulfodiimine inhibitor (1MMR), the water molecules corresponding to W1
283 and W2 are found [4].

284

285 3.5. Kinetic analysis of the MMP-7 variants

286

287 To see if the ionizable group responsible for pK_{e1} is Glu198, we constructed the
288 MMP-7 variant, E198A. To explore the possibility that either W1 or W2 is the ionizable
289 group responsible for pK_{e2} , we constructed the variants, A162G and P217G, assuming
290 that the main-chain structure of MMP-7 could be changed by mutating Ala162 or
291 Pro217 into glycine, which is the most flexible amino acid residue, and that such
292 mutation alters pK_{e2} if the ionizable group responsible for pK_{e2} is located in the
293 neighborhood of the site of mutation. The variants were produced in the *E. coli*
294 expression system [38]. The pH-dependence of the k_{cat}/K_m of the wild-type MMP-7,
295 E198A, A162G, and P217G in the hydrolysis of MOCAc-PLGL(Dpa)AR at 25°C is
296 shown in Fig. 6, and the kinetic parameters are summarized in Table 3. E198A

297 completely lacked the activity. To see if it retained small
298 MOCac-PLGL(Dpa)AR-hydrolyzing activity, we made HPLC analysis [27]. No
299 activity was detected in E198A even with the enzyme and substrate concentrations of 1
300 μM and 140 μM , respectively, and the reaction time of 120 min (data not shown). On
301 the other hand, the activity was detected in the wild-type enzyme with the enzyme and
302 substrate concentrations of 1 nM and 140 μM , respectively, and the reaction time of 10
303 min (data not shown). This indicated that the activity of E198A, if any, was less than
304 0.01% of that of the wild-type enzyme, suggesting that E198A completely lost the
305 activity and that Glu198 is not the ionizable group responsible for $\text{p}K_{\text{e}1}$.

306 A162G and P217G retained the activity with the $(k_{\text{cat}}/K_{\text{m}})_0$ values of 57% and 78%
307 of that of the wild-type enzyme, respectively (Table 3). The $\text{p}K_{\text{e}1}$ of A162G and P217G
308 were 4.9 ± 0.1 and 5.3 ± 0.1 , being higher by 0.3 ± 0.2 and 0.7 ± 0.2 unit, respectively,
309 than that of the wild-type enzyme (4.6 ± 0.1). The $\text{p}K_{\text{e}2}$ of A162G and P217G were 10.3
310 ± 0.1 and 10.0 ± 0.1 , being higher by 0.6 ± 0.2 and 0.3 ± 0.2 unit, respectively, than that
311 of the wild-type enzyme (9.7 ± 0.1). These results indicated that the mutations of
312 Ala162 \rightarrow Gly and Pro217 \rightarrow Gly affected the electrostatic environment of the ionizable
313 groups responsible for not only $\text{p}K_{\text{e}2}$ but also $\text{p}K_{\text{e}1}$.

314

315 **4. Discussion**

316

317 *4.1. Estimation of ionizable groups involved in the catalytic mechanism of MMP-7*

318

319 Browner et al. proposed that, based on the crystal structure of the complex of
320 MMP-7 and its inhibitor, Glu198 is the ionizable group responsible for $\text{p}K_{\text{e}1}$: it functions

321 both as a base and an acid, deprotonating the zinc-bound water and transferring the
322 proton to the leaving amine [4]. Cha et al. proposed that, based on the pH-dependence
323 of the activity, Tyr219 is the ionizable group responsible for pK_{e2} : the ionized side chain
324 of Tyr219 makes the active site of MMP-7 hydrophilic [25]. They also proposed that the
325 zinc-bound water, but not Glu198, is the ionizable group responsible for pK_{e1} : the
326 ionized zinc-bound water molecule attacks the carbonyl carbon of the scissile bond as a
327 nucleophile [26]. We demonstrated that, based on the results with chemical modification
328 [27] and site-directed mutagenesis [28], Tyr219 is not the ionizable group responsible
329 for pK_{e2} .

330 Thermodynamic analysis in this study suggested that glutamate residue is the
331 ionizable group for pK_{e1} , and that arginine or lysine residue is that for pK_{e2} (Tables 1
332 and 2). The mutation of Glu198→Ala completely abolished activity (Table 3). We think
333 that E198A has similar three-dimensional folds to the wild-type MMP-7 because the
334 expression level and stability of E198A were similar to those of the wild-type MMP-7:
335 starting from 100-ml culture, 2 mg purified E198A was obtained by the denaturation
336 and refolding processes. Purified E198A was stable on storage at 4°C. On the other
337 hand, some MMP-7 variants precipitated during the refolding process (K. Y. and K. I.,
338 unpublished data). Although it is difficult to exclude a possibility that the loss of activity
339 by the mutation Glu198→Ala does not result from the structural change, our result
340 suggests that Glu198 is the ionizable group responsible for pK_{e1} . This agrees well with
341 the previous reports that in MMP-1 [41], MMP-3 [42], and MMP-9 [43], the glutamate
342 residue corresponding to Glu198 of MMP-7 is catalytically important. On the other
343 hand, arginine and lysine residue were declined for the ionizable group for pK_{e2} because
344 there are no lysine or arginine residues in the active site. We therefore proposed that a

345 protein-bound water is the ionizable group for pK_{e2} . We noticed two water molecules,
346 Ala162-bound water (W1) and Pro217-bound water (W2), as the candidates for the
347 ionizable group for pK_{e2} . The mutations of Ala162→Gly and Pro217→Gly altered not
348 only pK_{e2} but also pK_{e1} values. This indicated that the mutations affected the
349 electrostatic environment of the active site. To further explore our hypothesis, extensive
350 site-directed mutagenesis study is required.

351

352 4.2. Catalytic mechanism of MMP-7

353

354 Based on the results in this study, we propose the following catalytic mechanism of
355 MMP-7 (Fig. 7). In free enzyme, Glu198 must be in its deprotonated state and the
356 protein-bound water must be in its unionized state for catalysis (Fig. 7A). The Michaelis
357 complex is formed when the carbonyl oxygen of the scissile bond binds the zinc ion.
358 Zinc ion polarizes the carbonyl group of the scissile bond. Glu198 accepts a proton from
359 the zinc-bound water (Fig. 7B). The tetrahedral complex is formed when the ionized
360 zinc-bound water attacks the carbonyl carbon of the scissile bond, and then stabilized by
361 the interaction between the carbonyl oxygen of the scissile bond and the oxygen of the
362 protein-bound water in its unionized state (Fig. 7C). This stabilization does not occur
363 when this protein-bound water is negatively charged. The amino product is released
364 when Glu198 transfers the proton to the nitrogen of the scissile bond (Fig. 7D).

365 pK_a of free water is 15.7. The above mechanism is consistent with the pH
366 dependence of MMP-7 activity with pK_{e1} and pK_{e2} values of 4.0 and 9.8 if the pK_a of
367 the protein-bound water greatly decreases. The zinc-bound water should be released in
368 the MMP-7-hydroxamate inhibitor complex (Protein Data Bank no. 1MMQ) [4]

369 because hydroxamate (R-CO-NH-OH) binds to the zinc ion as the bidentate ligand.
370 When the substrate coordinates to the zinc ion through the mono dentate ligand such as
371 the carbonyl oxygen of the scissile bond, it still binds to the zinc ion. Therefore, it is
372 thought that the pK_a of the zinc-bound water also greatly decreases. Considering the
373 mechanism that the ionized zinc-bound water attacks the carbonyl carbon of the scissile
374 bond (Fig. 7), it is thought that the ionizable group responsible for pK_{e2} is the
375 protein-bound, but not zinc-bound, water.

376 It should be mentioned that in MMP-3, the protein-bound water involved in the
377 catalytic mechanism was in its protonated state for catalysis, stabilizing the tetrahedral
378 intermediate by coordinating the carbonyl oxygen of the scissile bond of the substrate
379 [44]. In carboxypeptidase A, which belongs to Clan MC of zinc metalloproteinase, the
380 ionizable group for pK_{e1} of 7 was assigned to the active-site glutamate residue, and that
381 for pK_{e2} of 10 was assigned to the zinc-bound water molecule [45]. It was thought that
382 the active-site glutamate residue functions as a general base while the zinc-bound water
383 is in its unionized state, stabilizing the tetrahedral intermediate [45].

384

385 *4.3. Estimation of the ionizable groups involved in the catalytic mechanism of enzymes*
386 *by ΔH° of deprotonation*

387

388 pK_a of active-site residues can vary depending on their microenvironment. To our
389 knowledge, the highest pK_a of the active-site glutamate residue is 8.4 in xylanase [46],
390 suggesting that it is difficult to estimate the ionizable groups of enzymes only by their
391 pK_a values. In this study, we determined pK_a of side chains of L-Asp, L-Glu, L-His,
392 L-Cys, L-Tyr, L-Lys, and L-Arg at 25-45°C by the pH titration of amino-acid solutions,

393 from which we calculated ΔH^0 of deprotonation. In the previous reports [29], ΔH^0 of
394 side chains of L-Asp and L-Glu were the same (in the range of -6 to 6 kJ mol⁻¹). In this
395 study, they were different (-6.4 ± 3.5 kJ mol⁻¹ for L-Asp and -23.6 ± 5.8 kJ mol⁻¹ for
396 L-Glu) (Table 1). Considering that the ionizable group for pK_{e1} can be assigned to
397 Glu198 by the ΔH^0 value (-20.6 ± 6.1 kJ mol⁻¹), the ΔH^0 of side chains of amino acids
398 presented in this study might be a powerful tool to estimate the ionizable groups
399 involved in the catalytic mechanism of various enzymes.

400 In conclusion, we propose that Glu198 and unidentified protein-bound water are
401 the ionizable groups involved in the catalytic mechanism of MMP-7. To identify the
402 protein-bound water, site-directed mutagenesis study of MMP-7 is currently underway.

403

404 **Acknowledgements**

405

406 This study was supported in part (K. I.) by Grants-in-Aid for Scientific Research (Nos.
407 17380065 and 20380061) from the Japan Society of the Promotion of Science.

408

409 **References**

410

411 [1] J.F. Woessner, Jr., Matrix metalloproteinases and their inhibitors in connective tissue
412 remodeling. *FASEB J.* 5 (1991) 2145-2154.

413 [2] H. Nagase, J.F. Woessner, Jr., Matrix metalloproteinases. *J. Biol. Chem.* 274 (1999)
414 21491-21494.

415 [3] J.F. Woessner, Jr., C.J. Taplin, Purification and properties of a small latent matrix
416 metalloproteinase of the rat uterus. *J. Biol. Chem.* 263 (1988) 16918-16925.

- 417 [4] M.F. Browner, W.W. Smith, A.L. Castelhana, Matrilysin-inhibitor complexes:
418 common themes among metalloproteinases. *Biochemistry* 34 (1995) 6602-6610.
- 419 [5] N.D. Rawlings, F.R., Morton, C.Y. Kok, J. Kong, A.J. Barrett, MEROPS: the
420 peptidase database. *Nucleic Acids Res.* 36 (2008) D320-D325.
- 421 [6] W.-H. Yu, J.F. Woessner, Jr., Heparan sulfate proteoglycans as extracellular docking
422 molecules for matrilysin (matrix metalloproteinase 7). *J. Biol. Chem.* 275 (2000)
423 4183-4191.
- 424 [7] K. Yamamoto, S. Higashi, M. Kioi, J. Tsunozumi, K. Honke, K. Miyazaki, Binding
425 of active matrilysin to cell surface cholesterol sulfate is essential for its
426 membrane-associated proteolytic action and induction of homotypic cell adhesion. *J.*
427 *Biol. Chem.* 281 (2006) 9170-9180.
- 428 [8] S. Higashi, M. Oeda, K. Yamamoto, K. Miyazaki, Identification of amino acid
429 residues of matrix metalloproteinase 7 essential for binding to cholesterol sulfate. *J.*
430 *Biol. Chem.* 283 (2008) 35735-35744.
- 431 [9] K. Yamamoto, K. Miyazaki, S. Higashi, Cholesterol sulfate alters substrate
432 preference of matrix metalloproteinase-7 and promotes degradations of pericellular
433 laminin-332 and fibronectin. *J. Biol. Chem.* 285 (2010) 28862-28873.
- 434 [10] C.C. Lynch, T. Vargo-Gogola, M.D. Martin, B. Fingleton, H.C. Crawford, L.M.
435 Matrisian, Matrix metalloproteinase 7 mediates mammary epithelial cell tumorigenesis
436 through the ErbB4 receptor. *Cancer Res.* 57 (2007) 6760-6767.
- 437 [11] H. Oneda, M. Shihara, K. Inouye, Inhibitory effects of green tea catechins on the
438 activity of human matrix metalloproteinase 7 (matrilysin). *J. Biochem.* 133 (2003)
439 571-576.
- 440 [12] Y. Muta, S. Oyama, T. Umezawa, M. Shimada, K. Inouye, Inhibitory effects of

441 lignans on the activity of human matrix metalloproteinase 7 (matrilysin). *J. Agric. Food*
442 *Chem.* 52 (2004) 5888-5894.

443 [13] H. Oneda, K. Inouye, Interactions of human matrix metalloproteinase 7
444 (matrilysin) with the inhibitors thiorphan and R-94138. *J. Biochem.* 129 (2001)
445 429-435.

446 [14] H.I. Park, S. Lee, A. Ullah, Q. Cao, Q.X. Sang, Effects of detergents on catalytic
447 activity of human endometase/matrilysin 2, a putative cancer biomarker. *Anal. Biochem.*
448 396 (2010) 262-268.

449 [15] T. Crabbe, F. Willenbrock, D. Eaton, P. Hynds, A.F. Carne, G. Murphy, A.J.
450 Docherty, Biochemical characterization of matrilysin. Activation conforms to the
451 stepwise mechanisms proposed for other matrix metalloproteinases. *Biochemistry* 31
452 (1992) 8500-8507.

453 [16] G.I. Goldberg, S.M. Wilhelm, A. Kronberger, E.A. Bauer, G.A. Grant, A.Z. Eisen,
454 Human fibroblast collagenase. Complete primary structure and homology to an
455 oncogene transformation-induced rat protein. *J. Biol. Chem.* 261 (1986) 6600-6605.

456 [17] B. Birkedal-Hansen, W.G. Moore, R.E. Taylor, A.S. Bhowan, H. Birkedal-Hansen,
457 Monoclonal antibodies to human fibroblast procollagenase. Inhibition of enzymatic
458 activity, affinity purification of the enzyme, and evidence of clustering epitopes in the
459 NH₂-terminal end of the activated enzyme. *Biochemistry* 27 (1988) 6751-6758.

460 [18] S.E. Whitham, G. Murphy, P. Angel, H.J. Rahmsdorf, B.J. Smith, A. Lyons, T.J.
461 Harris, J.J. Reynolds, P. Herrlich, A.J. Docherty, Comparison of human stromelysin and
462 collagenase by cloning and sequence analysis. *Biochem. J.* 240 (1986) 913-916.

463 [19] D. Muller, B. Quantin, M.C. Gesnel, R. Millon-Collard, J. Abecassis, R.
464 Breathnach, The collagenase gene family in humans consists of at least four members.

465 Biochem. J. 253 (1988) 187-192.

466 [20] P. Devarajan, K. Mookhtiar, H. van Wart, N. Berliner, Structure and expression of
467 the cDNA encoding human neutrophil collagenase. *Blood* 77 (1991) 2731-2738.

468 [21] H. Birkedal-Hansen, W.G. Moore, M.K. Bodden, L.J. Windsor, B. Birkedal-Hansen,
469 A. DeCarlo, J.A. Engler, Matrix metalloproteinases: a review. *Crit. Rev. Oral Biol. Med.*
470 4 (1993) 197-250.

471 [22] P. Basset, J.P. Bellocq, C. Wolf, I. Stoll, P. Hutin, J.M. Limacher, O.L. Podhajcer,
472 M.P. Chenard, M.C. Rio, P. Chambon, A novel metalloproteinase gene specifically
473 expressed in stromal cells of breast carcinomas. *Nature* 348 (1990) 699-704.

474 [23] T. Takino, H. Sato, E. Yamamoto, M. Seiki, Cloning of a human gene potentially
475 encoding a novel matrix metalloproteinase having a C-terminal transmembrane domain.
476 *Gene* 155 (1995) 293-298.

477 [24] Q.A. Sang, D.A. Douglas, Computational sequence analysis of matrix
478 metalloproteinase. *J. Protein Chem.* 15 (1996) 137-160.

479 [25] J. Cha, M.V. Pedersen, D.S. Auld, Metal and pH dependence of heptapeptide
480 catalysis by human matrilysin. *Biochemistry* 35 (1996) 15831-15838.

481 [26] J. Cha, D.S. Auld, Site-directed mutagenesis of the active site glutamate in human
482 matrilysin: investigation of its role in catalysis. *Biochemistry* 36 (1997) 16019-16024.

483 [27] Y. Muta, H. Oneda, K. Inouye, Anomalous pH-dependence of the activity of human
484 matrilysin (matrix metalloproteinase-7) as revealed by nitration and amination of its
485 tyrosine residues. *Biochem. J.* 386 (2005) 263-270.

486 [28] Y. Muta, K. Inouye, Tyr219 of human matrix metalloproteinase 7 (MMP-7) is not
487 critical for catalytic activity, but is involved in the broad pH-dependence of the activity.
488 *J. Biochem.* in press

489 [29] J.T. Edsall, Dipolar ions and acid-base equilibria in: E.J. Cohn, J.T. Edsall (Eds.),
490 Proteins, amino acids, and peptides as ions and dipolar ions, Hafner Publishing
491 Company, New York and London, 1943, pp. 75-115.

492 [30] J.P. Geenstein, Studies of the peptides of trivalent amino acids. I. Titration
493 constants of histidyl-histidine and of aspartyl-aspartic acid. J. Biol. Chem. 93 (1931)
494 479-494.

495 [31] J.P. Greenstein, Studies of the peptides of trivalent amino acids. III. The apparent
496 dissociation constants, free energy changes, and heats of ionization of peptides
497 involving arginine, histidine, lysine, tyrosine, and aspartic and glutamic acids, and the
498 behavior of lysine peptides toward nitrous acid. J. Biol. Chem. 101 (1933) 603-621.

499 [32] P.K. Smith, A.C. Taylor, E.R.B. Smith, Thermodynamic properties of solutions of
500 amino acids and related substances. III. The ionization of aliphatic amino acids in
501 aqueous solution from one to fifty degrees. J. Biol. Chem. 122 (1937) 109-123.

502 [33] R. Cecil, J.R. McPhee, A kinetic study of the reactions on some disulphides with
503 sodium sulphite. Biochem. J. 60 (1955) 496-506.

504 [34] K. Hiromi, K. Takahashi, Z. Hamauzu, S. Ono, Kinetic studies on gluc-amylase.
505 III. The influence of pH on the rates of hydrolysis of maltose and panose. J. Biochem.
506 59 (1966) 469-475.

507 [35] W.J. Zhu, M. Li, X.Y. Wang, Chemical modification studies on arginine kinase:
508 essential cysteine and arginine residues at the active site. Int. J. Biol. Macromol. 41
509 (2007) 564-571.

510 [36] M.Y. Kondo, D.N. Okamoto, J.A. Santos, M.A. Juliano, K. Oda, B. Pillai, M.N.
511 James, L. Juliano, I.E. Gouvea, Studies on the catalytic mechanism of glutamic
512 peptidase. J. Biol. Chem. 285 (2010) 21437-21445.

513 [37] C.G. Knight, F. Willenbrock, G. Murphy, A novel coumarin-labelled peptide for
514 sensitive continuous assays of the matrix metalloproteinase. FEBS Lett. 296 (1992)
515 263-266.

516 [38] Y. Muta, N. Yasui, Y. Matsumiya, M. Kubo, K. Inouye, Expression in *Escherichia*
517 *coli*, refolding, and purification of the recombinant mature form of human matrix
518 metalloproteinase 7 (MMP-7). Biosci. Biotechnol. Biochem. 74 (2010) 2151-2517.

519 [39] H. Oneda, K. Inouye, Refolding and recovery of recombinant human matrix
520 metalloproteinase 7 (matrilysin) from inclusion bodies expressed by *Escherichia coli*. J.
521 Biochem. 126 (1999) 905-911.

522 [40] M. Betz, P. Huxley, S.J. Davies, Y. Mushtaq, M. Pieper, H. Tschesche, W. Bode,
523 F.X. Comis-Rüth, 1.8-Å crystal structure of the catalytic domain of human neutrophil
524 collagenase (matrix metalloproteinase-8) complexed with a peptidomimetic
525 hydroxamate primed-side inhibitor with a distinct selectivity profile. Eur. J. Biochem.
526 247 (1997) 356-363.

527 [41] L.J. Windsor, M.K. Bodden, B. Birkedal-Hansen, J.A. Engler, H. Birkedal-Hansen,
528 Mutational analysis of residues in and around the active site of human fibroblast-type
529 collagenase. J. Biol. Chem. 269 (1994) 4033-4040.

530 [42] B. Arza, M. de Maeyer, J. Félez, D. Collen, H.R. Lijnen, H.R. (2001) Critical role
531 of glutamic acid 202 in the enzyme activity of stromelysin-1 (MMP-3). Eur. J. Biochem.
532 268 (2001) 826-831

533 [43] S. Rowsell, P. Hawtin, C.A. Minshull, H. Jepson, S.M. Brockbank, D.G. Barratt,
534 A.M. Slater, W.L. McPheat, D. Waterson, A.M. Henney, R.A. Pauptit, Crystal structure
535 of human MMP9 in complex with a reverse hydroxamate inhibitor. J. Mol. Biol. 319
536 (2002) 173-181.

537 [44] V. Pelmeshnikov, P.E. Siegbahn, Catalytic mechanism of matrix
538 metalloproteinases: two-layered ONIOM study. *Inorg. Chem.* 41 (2002) 5659-5666.

539 [45] K. Zhang, D.S. Auld, Structure of binary and ternary complexes of zinc and cobalt
540 carboxypeptidase A as determined by X-ray absorption fine structure. *Biochemistry* 34
541 (1995) 16306-16312.

542 [46] M.D. Joshi, G. Sidhu, I. Pot, G.D. Brayer, S.G. Withers, L.P. McIntosh, Hydrogen
543 bonding and catalysis: a novel explanation for how a single amino acid substitution can
544 change the pH optimum of a glycosidase. *J. Mol. Biol.* 299 (2000) 255-279.

545

546 **Figure Legends**

547

548 Fig. 1. Structure of MMP-7. The MMP-7-hydroxamate inhibitor complex (Protein Data
549 Bank no. 1MMQ) [4] was drawn using Swiss-Pdb Viewer 4.0. The active-site zinc ion is
550 shown as a sphere. (A) Overall structure. Peptide chain is represented by a ribbon. The
551 side chains of Glu198, Tyr193, Tyr216, and Tyr219 and the hydroxamate inhibitor are
552 shown as a stick. (B) Close-up view of the active site. The side chains of Glu198 and
553 Tyr219, the main and side chains of Ala162 and Pro217, and the two water molecules
554 (W1 and W2) are shown as a ball and stick. The hydroxamate inhibitor is shown as a
555 wire with the nearest two oxygen atoms to the active-site zinc ion as a ball. The number
556 indicates that of the amino acid residues.

557

558 Fig. 2. Reaction scheme for the pH-dependence of MMP-7 activity with two ionizable
559 groups involved in enzyme activity. E, S, H, and P denote MMP-7, the substrate, proton,
560 and the product, respectively. K_{e1} and K_{e2} are proton dissociation constants of the
561 ionizable groups of the free MMP-7, respectively, and K_{es1} and K_{es2} are proton
562 dissociation constants of the MMP-7 combined with substrate, respectively [27,34].

563

564 Fig. 3. Titration curve of pH of L-Glu solution. The titration was carried out at 25 (open
565 circle), 35 (open square), and 45°C (open triangle). The degree of dissociation of L-Glu
566 at each pH was calculated by Eq. 7. The pK_{a1} and pK_{a2} were calculated by Eq. 10, which
567 were 2.1 ± 0.1 and 4.0 ± 0.1 for 25°C, 2.2 ± 0.1 and 4.1 ± 0.1 for 35°C, and 2.3 ± 0.1
568 and 4.2 ± 0.1 for 45°C, respectively. Inset shows van't Hoff plot for pK_{a2} of L-Glu.
569 Enthalpy change, ΔH° , of deprotonation was calculated to be $-23.6 \pm 5.8 \text{ kJ mol}^{-1}$. One
570 of the representative data is shown.

571

572 Fig. 4. Effect of pH on the wild-type MMP-7-catalyzed hydrolysis of
573 MOCAc-PLGL(Dpa)AR. The reaction was carried out at 15 (open circle), 25 (open
574 square), 35 (open triangle), and 45°C (open diamond), each with the initial enzyme and
575 substrate concentrations of 10 nM and 1.5 μM, respectively. The relative k_{cat}/K_m is
576 defined as the ratio of the k_{cat}/K_m at the indicated pH to that at the optimal pH ($1.63 \times$
577 $10^{-4} \text{ M}^{-1} \text{ s}^{-1}$ at pH 6.8 for 15°C, $4.01 \times 10^{-4} \text{ M}^{-1} \text{ s}^{-1}$ at pH 6.8 for 25°C, $5.39 \times 10^{-4} \text{ M}^{-1} \text{ s}^{-1}$
578 at pH 6.6 for 35°C, and $7.77 \times 10^{-4} \text{ M}^{-1} \text{ s}^{-1}$ at pH 6.0 for 45°C). Error bars indicate SD
579 values. One of the representative data is shown.

580

581 Fig. 5. van't Hoff plot for pK_e of MMP-7. pK_{e1} (A) and pK_{e2} (B) values of MMP-7 were
582 plotted against the reciprocal of the absolute temperature. Error bars indicate SD values.
583 Enthalpy change, ΔH° , of deprotonation was calculated from the slope: (A) -20.6 ± 6.1
584 kJ mol^{-1} ; (B) $89.9 \pm 4.0 \text{ kJ mol}^{-1}$. One of the representative data is shown.

585

586 Fig. 6. Effect of pH on the MMP-7 variants-catalyzed hydrolysis of
587 MOCAc-PLGL(Dpa)AR at 25°C. The reaction was carried out with the wild-type
588 MMP-7 (open circle), A162G (open square), and P217G (open triangle). The initial
589 enzyme and substrate concentrations were 10 nM and 1.5 μM, respectively. The relative
590 k_{cat}/K_m is defined as the ratio of the k_{cat}/K_m at the indicated pH to that at the optimal pH
591 ($4.01 \times 10^{-4} \text{ M}^{-1} \text{ s}^{-1}$ at pH 6.8 for the wild-type MMP-7, $2.46 \times 10^{-4} \text{ M}^{-1} \text{ s}^{-1}$ at pH 6.8 for
592 A162G, and $3.18 \times 10^{-4} \text{ M}^{-1} \text{ s}^{-1}$ at pH 7.0 for P217G). Error bars indicate SD values. One
593 of the representative data is shown.

594

595 Fig. 7. Proposed mechanism for the MMP-7-catalyzed cleavage of peptides. See the text

596 for details.

597

A

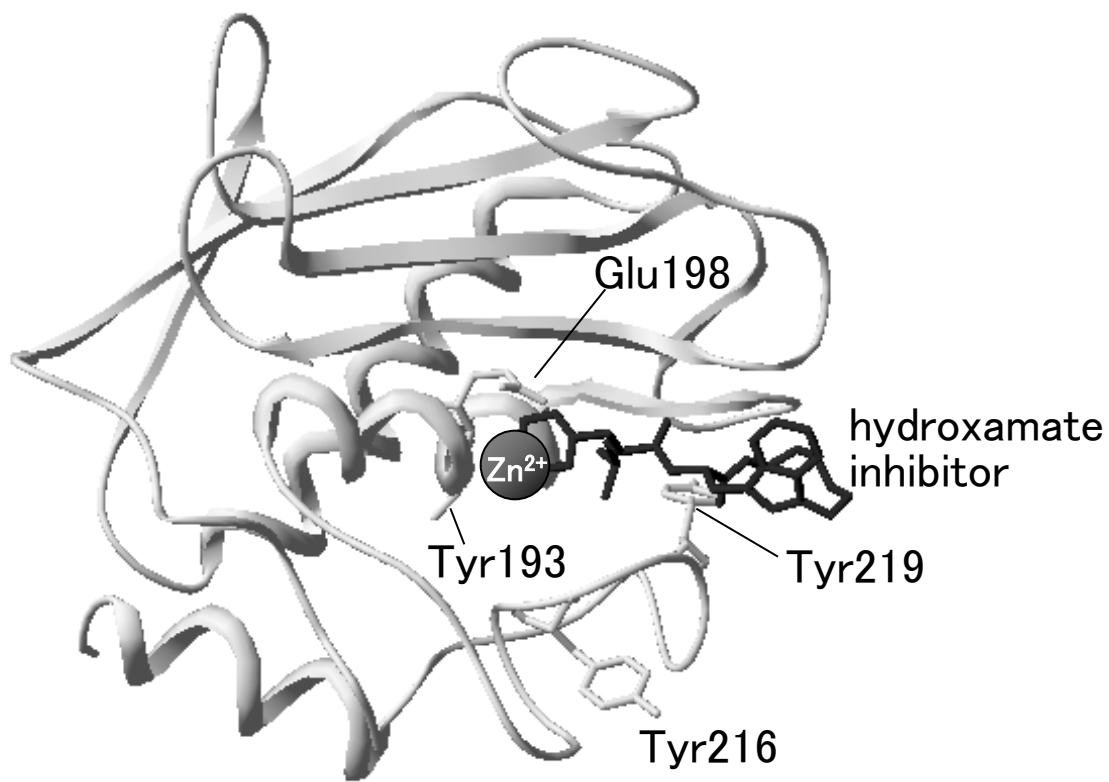


Fig. 1

B

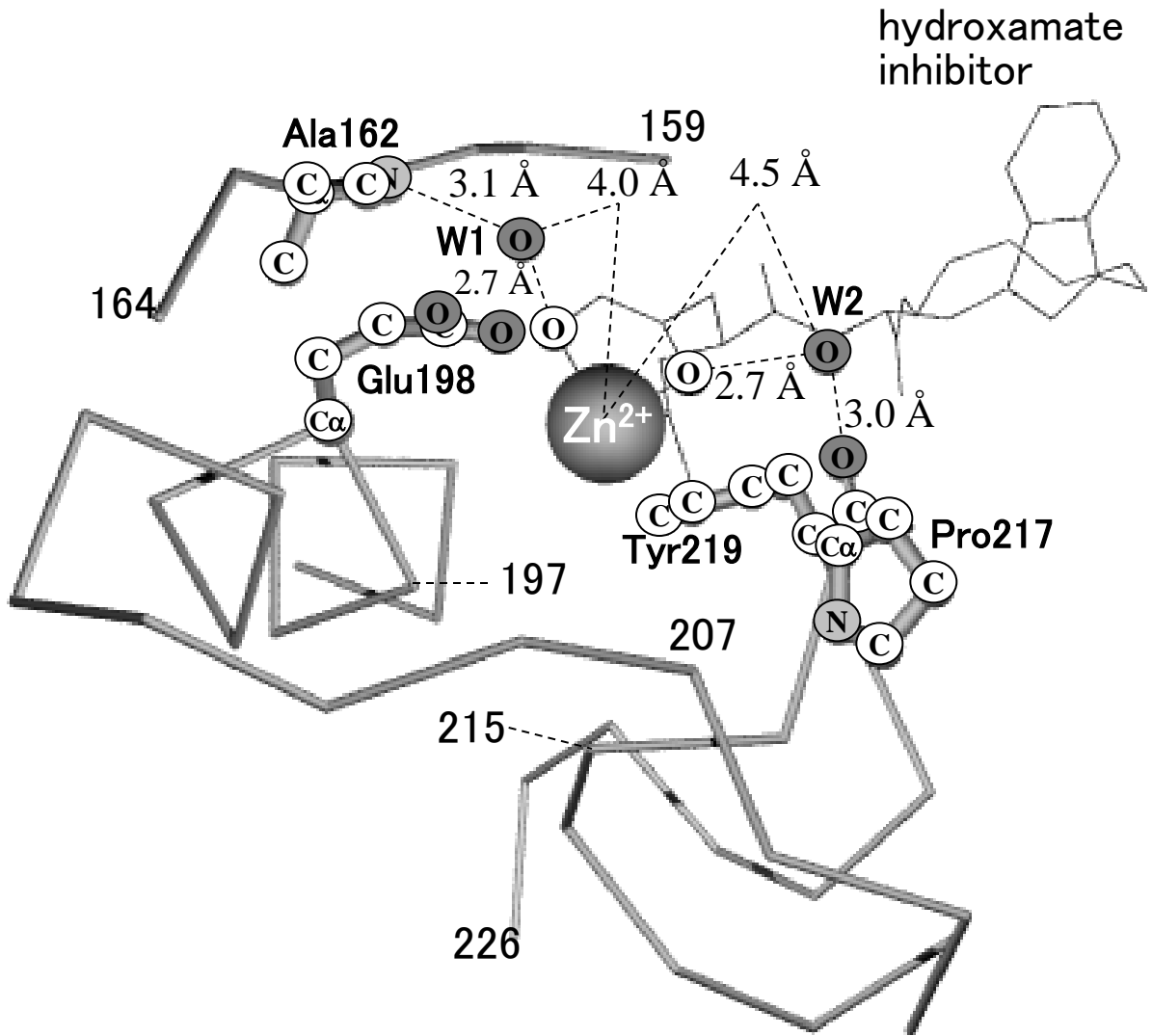
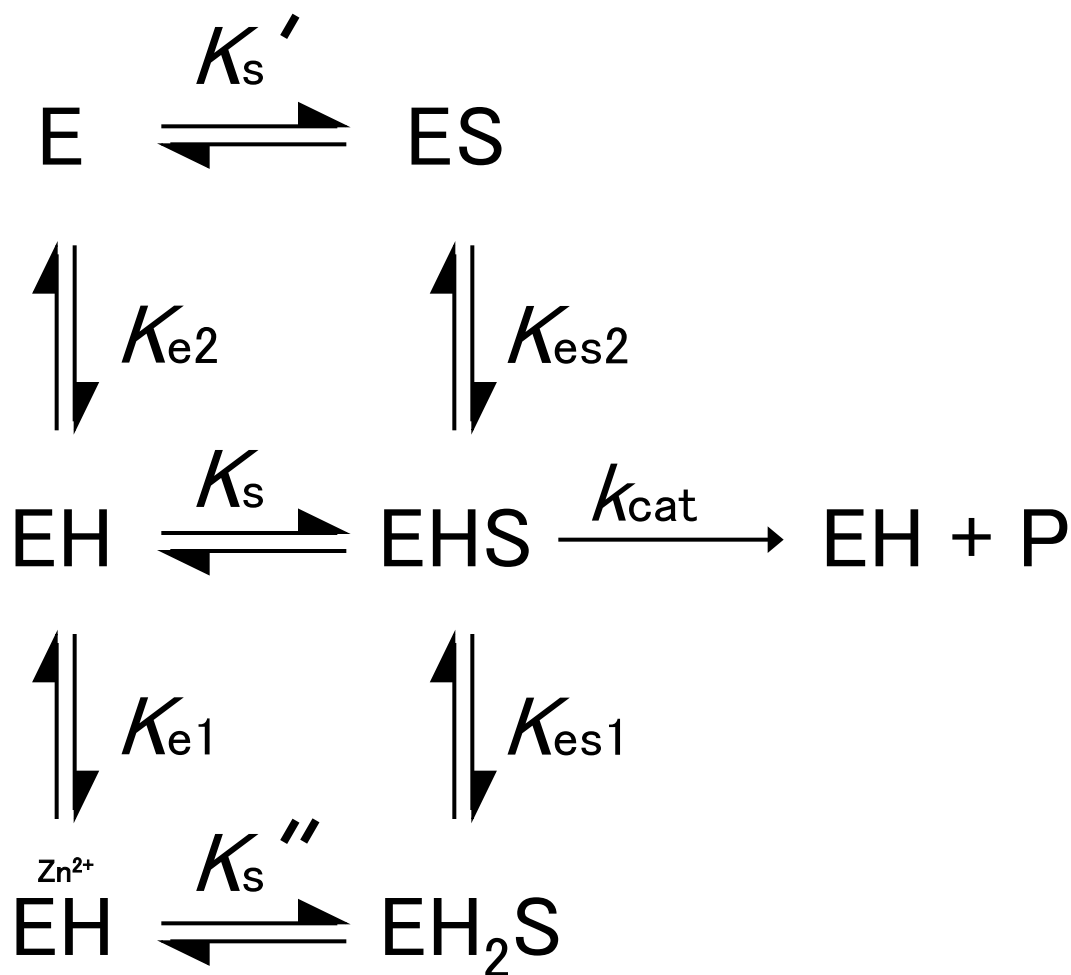


Fig. 1



2

Fig. 2

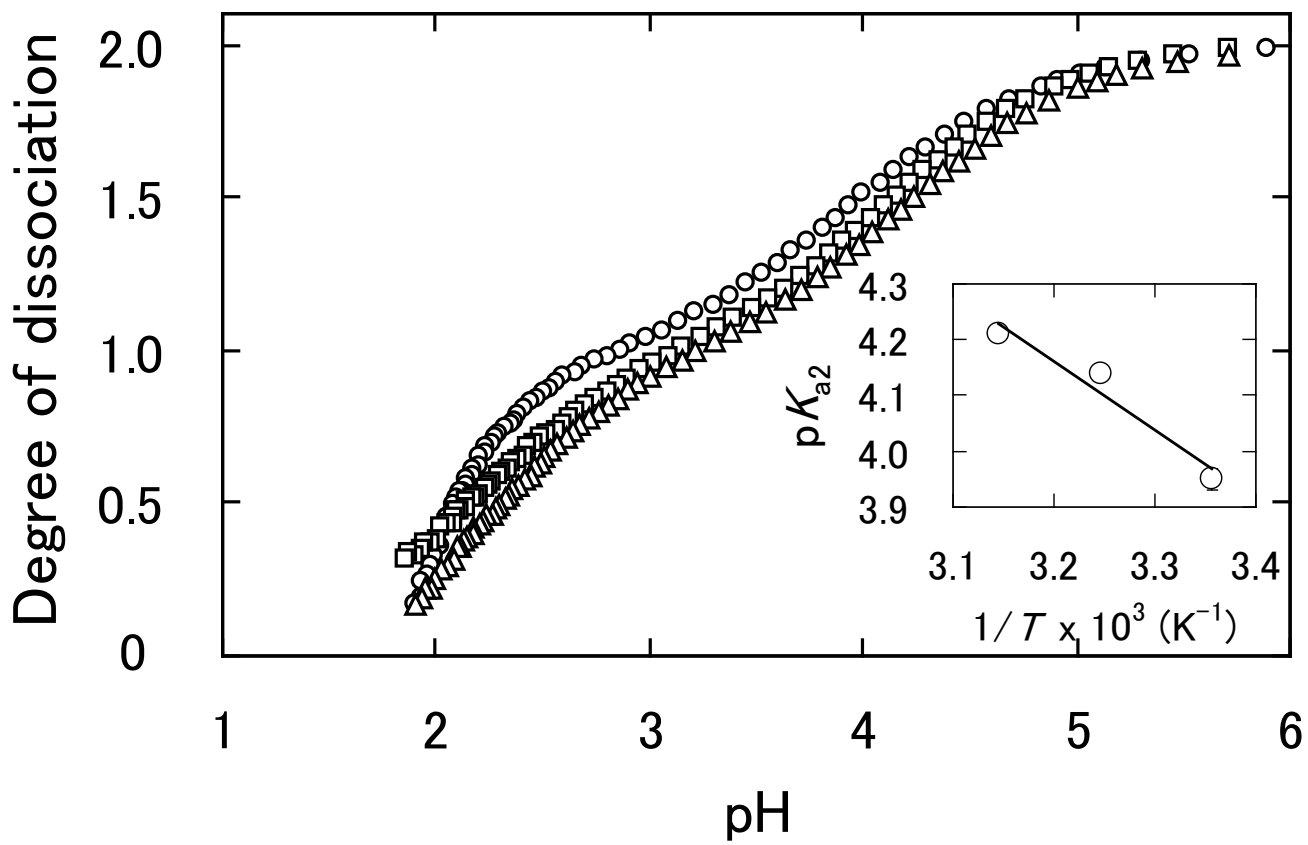


Fig. 3

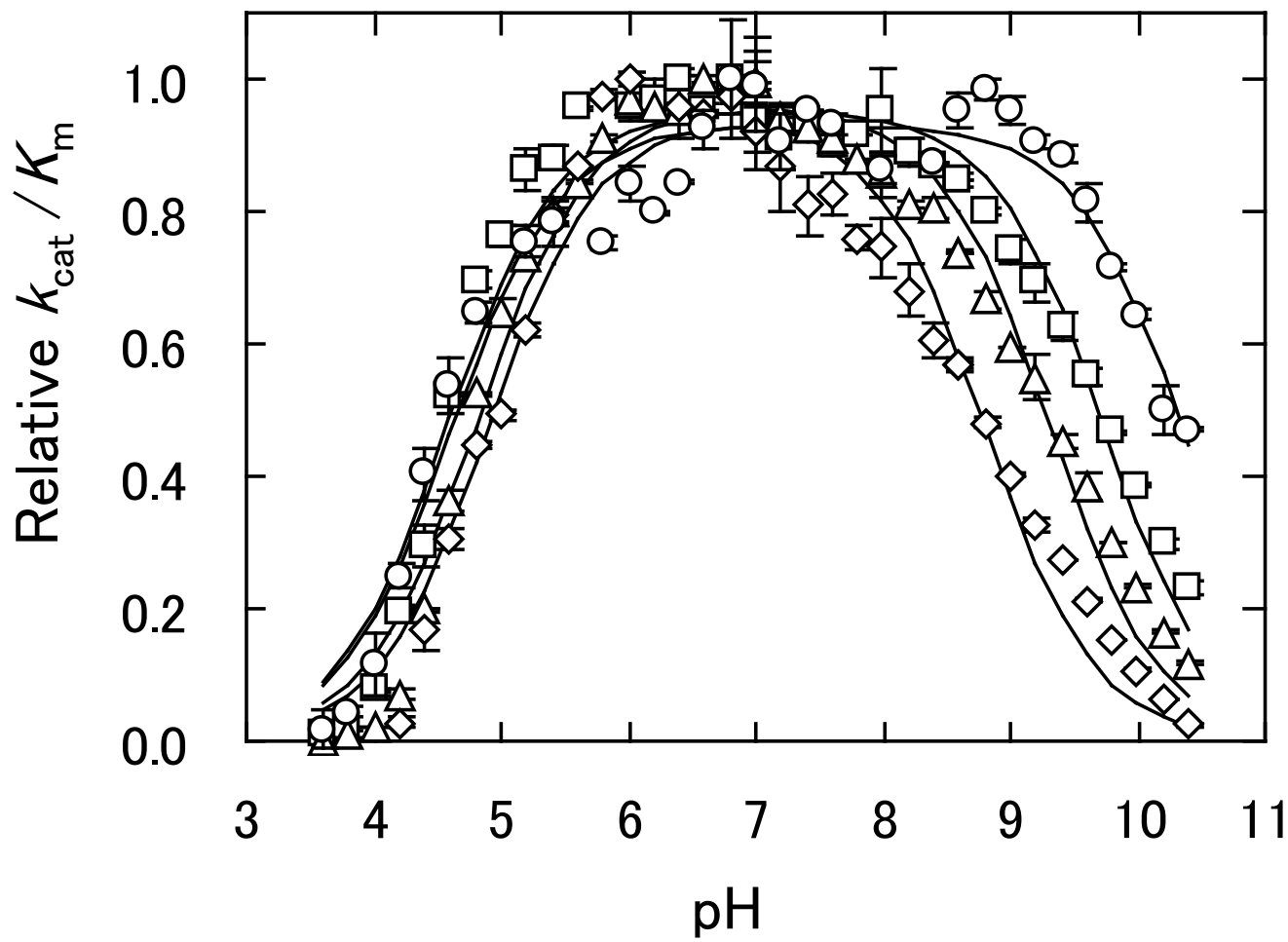


Fig. 4

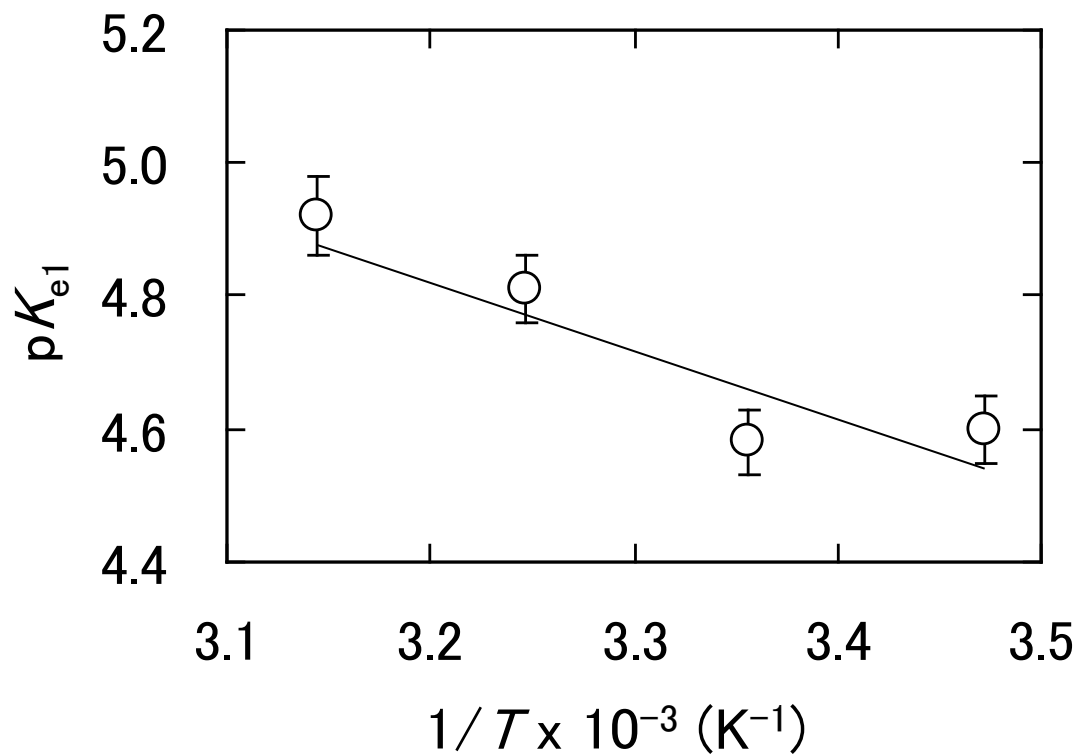
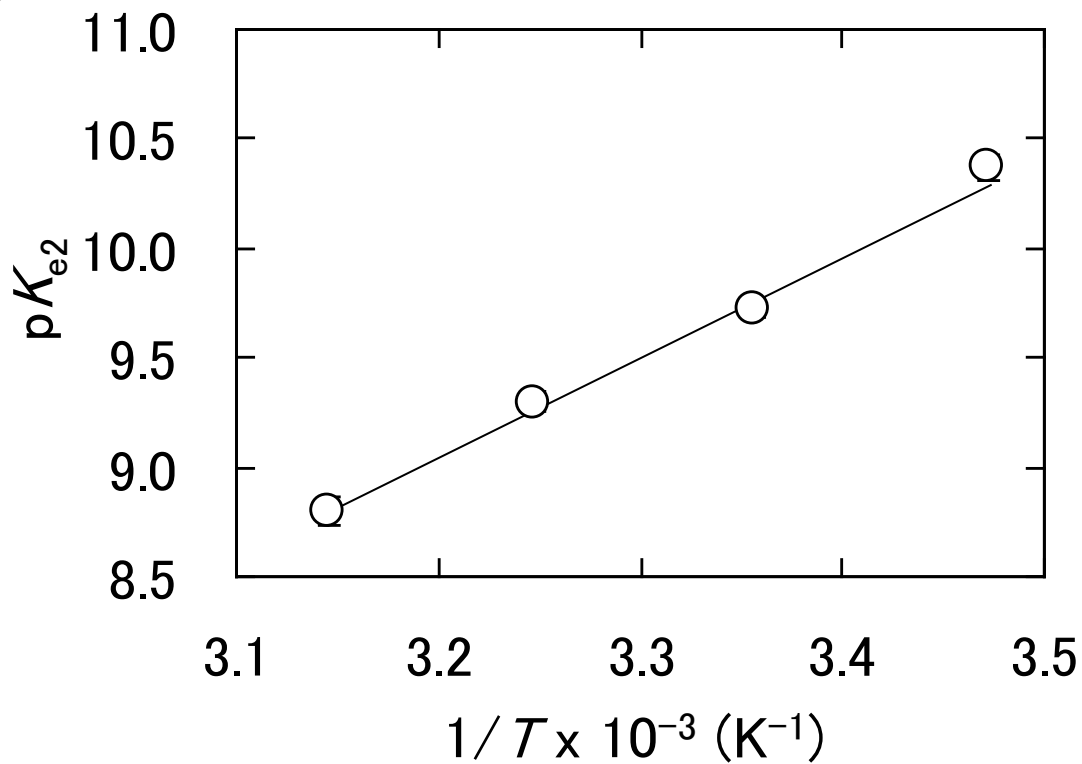
A**B**

Fig. 5

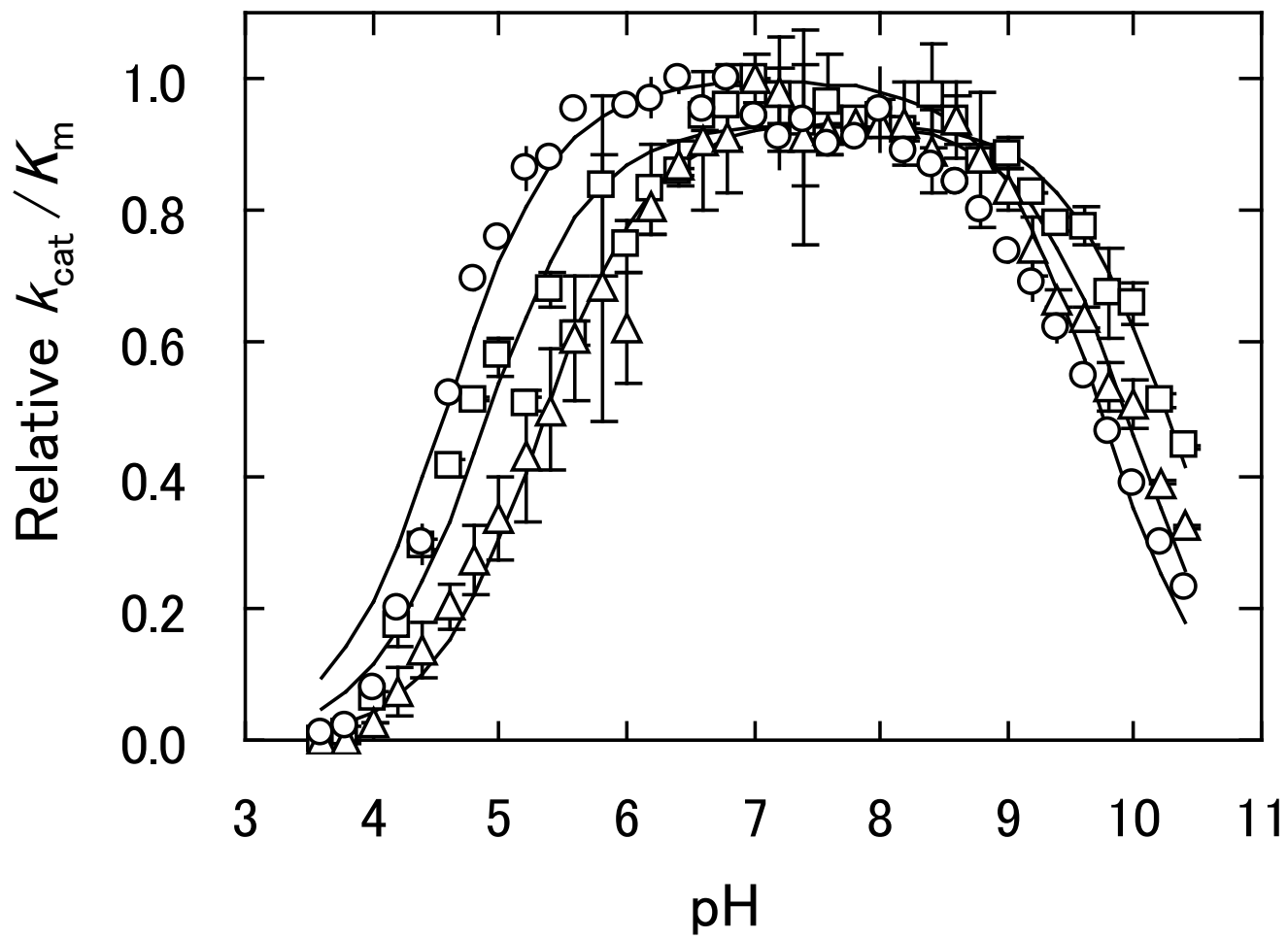


Fig. 6

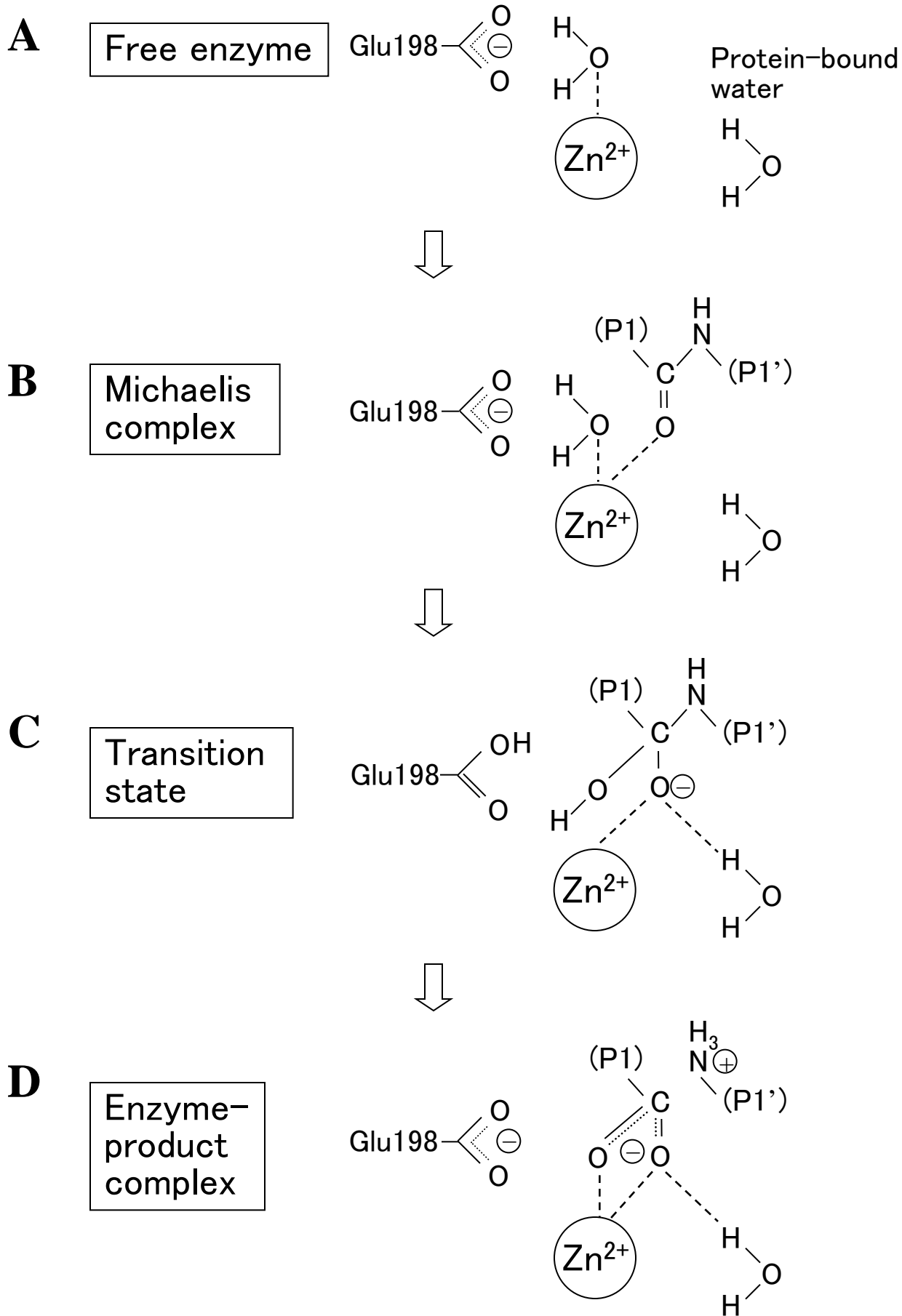


Fig. 7